Large-eddy simulation of sheared interfacial flow

S. Reboux, P. Sagaut,[a] and D. Lakehal[b]
Institute of Energy Technology, ETH Zurich, Zurich CH-8092, Switzerland

(Received 6 December 2005; accepted 31 August 2006; published online 16 October 2006)

Large-eddy simulations (LES) of a turbulent interfacial gas-liquid flows are described in this paper. The variational multiscale approach (VMS) introduced by Hughes for single-phase flows is systematically assessed against direct numerical simulation (DNS) data obtained at a shear Reynolds number $Re_\star = 171$, and compared to LES results obtained with the Smagorinsky model, modified by a near-interface turbulence decay treatment. The models are incorporated in the same pseudospectral DNS solver built within the *boundary fitting* method used by Fulgosi *et al.* for air-water flow. The LES are performed for physical conditions allowing low interface deformations that fall in the range of capillary waves of wave slope $ak=0.01$. The LES results show that both the modified Smagorinsky model and the VMS are capable to predict the boundary layer structure in the gas side, including the decay process, and to cope with the anisotropy of turbulence in the liquid blockage layer underneath the interface. Higher-order turbulence statistics, including the transfer of energy between the normal stresses is also well predicted by both approaches, but qualitatively the VMS results remain overall better than the modified Smagorinsky model. The study has demonstrated that the key to the prediction of the energy transfer mechanism is in the proper prediction of the fluctuating pressure field, which has been found out of reach of any of the LES methodologies. The superiority of the VMS is demonstrated through the analysis of the subgrid transport and exchange terms in the resolved kinetic energy, where it is indeed shown to be self-adaptive with regard to the eddy viscosity. Although VMS is shown to be sensitive to filter scale partition and model constant, the optimal setting can be easily translated in the interface tracking/finite-volume context, which makes it very useful for practical purposes. An important point is that the VMS approach yields very satisfactory results without the need for prescribing an ad-hoc damping function and the required distance to the interface. © *2006 American Institute of Physics*. [DOI: 10.1063/1.2359745]

I. INTRODUCTION

The interplay between turbulence structures and surface related scales in interfacial multifluid flows cannot be elucidated without the help of direct numerical simulation (DNS), and to a certain extent large-eddy simulation (LES). Interfacial flows are fluid systems involving immiscible, sheared streams separated by a well-defined continuous interface, such as stratified pipe flows or seawater waves with imposed wind shear. These flows involve different turbulence dynamics on each side of the interface; emphasis is then placed on predicting both turbulence and topology dynamics down to the interface level for each phase.

The sheared interfacial flow considered here differs from free surface turbulence abundantly studied hitherto,[4–6] in that it mimics the scenario of waves starting to form under the action of the imposed shear. If the structure of turbulence near the interface has characteristics somewhat similar to that of wall turbulence,[3] liquid-controlled transport processes should, however, be different from stress-free surface flows, because the turbulence structure is now controlled by generation in the near-interface region, and not from the farfield. A complication arises at a deformable interface in comparison to a rigid boundary in that part of the energy transferred from the gas to the water goes to generate waves, and part to generate turbulence directly.

The investigation of higher Reynolds number flows requires the use of LES, where only the large-scale motions (GS) are directly resolved. Despite the simple topology of the present flow, it actually involves various critical aspects that need to be carefully considered. The simulation methodology used should, for instance, be strictly conservative with regard to the transported quantities as the interface deforms. Further, the SGS model employed in both phases should be capable of restoring the main features of small-scale turbulence near the interface, namely, to accommodate the asymptotic behavior of turbulence, and to mimic the forward and backward transfer of kinetic energy, if it exists. A spurious dissipative behavior near the interface would otherwise smooth the interface resolution, affecting, in turn, the interphase exchange mechanisms. This is the reason why the assessment of the SGS models presented here is performed using the same DNS pseudospectral code, in which the interface deformations are simulated by the Boundary-Fitting method. The DNS database for the stratified air-water flow studied by Fulgosi *et al.*[3] is selected for comparison.

Our previous attempts to predict a stratified, sheared air-liquid flow using LES within the eddy-viscosity SGS modeling context have revealed the necessity to accommodate

[a]Also at the Laboratoire de Modélisation en Mécanique, Université Pierre et Marie Curie—Paris 6, Paris, France.
[b]Author to whom correspondence should be addressed. Also at ASCOMP GmbH. Telephone: +41 44 6327073. Fax: +41 6331662. Electronic mail: lakehal@iet.mavt.ethz.ch

the asymptotic behavior of turbulence near interfaces, like in wall flows.[2] The Smagorinsky model alone (referred to here as the reference Smagorinsky model) was too dissipative. Shen *et al.*[5] report also on the necessity of introducing a similar treatment near free surfaces (seen from the liquid side). This is, in principle, equivalent, since the continuity of stresses across the interface should reflect the decay of eddy viscosity imposed on the gas to the liquid. To apply the model proposed in Ref. 2 for practical applications (using finite volume solvers), an algorithm has been recently developed by Liovic and Lakehal[7] in which the distance to the interface is first reconstructed from VOF data, then the frictional velocity is estimated at the interface to define a turbulence damping function. This strategy has been proven very tedious for three-dimensional flows featuring strong topology changes. Further, our experience with the dynamic approach based on the Germano[8] identity has not been fruitful in the sheared gas-liquid flow context, similar to the reports from Salvetti *et al.*[6] about the LES of free-surface flow. It is therefore legitimate to explore other ways of modeling the under-resolved scales for this class of flow, that dispense with near-interface turbulence treatment. This is our main motivation in this paper.

The variational multiscale approach (VMS) was first introduced by Hughes in a general framework for computational mechanics, and then applied to turbulent fluid flows[1,9] for SGS modeling. Several strategies have been proposed within the VMS framework: Hughes *et al.*[1,9,10] originally use truncation on a pseudospectral basis, cell clustering was adopted by Koobus and Farhat,[11] equivalent hyperviscosity formulation was analyzed by Sagaut and Levasseur,[12] and a generalized filtering formulation was developed by Vreman.[13]

Numerical experiments in wall bounded flows have shown the VMS approach to lead to the definition of self-adaptive SGS models, similar to the dynamic strategy based on the Germano identity. This means that it should virtually dispense with near-wall turbulence treatment, which stimulates its extension for interfacial flows. Specifically, the velocity field is partitioned into coarse-scale (low wavenumber) and fine-scale (high wavenumber) components. The subgrid scale stress is thus made a function of the fine-scale velocity field, and applies only to the fine-scale motions, meaning that energy is extracted only from high wavenumber modes. Extracting energy solely from high wavenumber modes is precisely what makes the formulation outperform conventional LES models, which extract energy from all modes.[14] The conventional dynamic model yields an eddy viscosity with too much activity in the large scales.[15] The multiscale implementation avoids this difficulty by applying the eddy viscosity only to the small-scale portion of the spectrum. However, it is unable to represent the long-range transfer of energy from the low wavenumber modes to the subgrid scales. While this may be negligible for highly resolved LES, where the scale separation is large and the strain rate magnitude of large scales is relatively small, the effect may be appreciable for large enough filter sizes, or coarse LES.[14]

In the present paper we address the application of the VMS approach to sheared interfacial two-phase flows, placing the emphasis on its behavior near the interface. To this end both *a priori* and *a posteriori* tests are carried out and results are compared against existing DNS data, and compared to a set of LES results obtained with Smagorinsky-based SGS models, with and without near-interface treatment.

The paper is organized as follows. The main features of the reference DNS are recalled in Sec. II. Governing equations of the LES problem, including the interface treatment and the selected VMS closure, are discussed in Sec. III. This section includes the analysis of the sensitivity of the results to details of the VMS closure as well. An extensive analysis of filtered LES results using the SGS model of reference and its modified version is presented in Sec. IV. The VMS results are discussed in Sec. V, and conclusions are presented in Sec. VI.

II. DNS OF TURBULENCE AT A SHEARED GAS-LIQUID INTERFACE

The flow investigated is well described by Fulgosi *et al.*[3] It involves turbulent air and water streams flowing in opposite directions at the same shear Reynolds number, $\mathrm{Re}_\star = u_\star 2h/\nu = 171$. The flow quantities normalized by the inner variables, namely the shear velocity $u_\star = \sqrt{\tau_{\mathrm{int}}/\rho}$, where τ_{int} represents the shear stress at the interface, the half-depth of each computational domain h, and the kinematic viscosity ν. The flow in each subdomain is driven by a constant pressure gradient Π, such that $u_\star = \sqrt{2h\Pi/\rho}$. The sheared interface is allowed to deform in space and time by solving a convection equation for the surface elevation. When the interface is flat, the interfacial shear balances the imposed mean pressure gradient. As the interfacial waves start to develop, part of the energy is transferred into form drag, leading to a reduction of the interfacial shear. The nondimensional time is defined by $t^+ = t\nu/u_\star^2$ in wall units, or by $t_{\mathrm{ls}} = tU_0/h$ in large-scale units, where U_0 is the mean streamwise velocity. With these reference quantities $(u_\star, \nu/u_\star^2, h)$, the Navier-Stokes equations for the incompressible, isothermal, Newtonian fluids flowing in the two subdomains are nondimensionalized as follows: the velocity vector $\mathbf{u}$ is made nondimensional by the reference velocity $u_\star$, and the dynamic pressure p is normalized by $\rho u_\star^2$. In the absence of mass transfer, the gas and liquid phases are explicitly coupled at the interface by the continuity of velocities and shear stresses:

$$\frac{1}{\mathrm{Re}_\star}[(\underline{\underline{\tau}}_L - \underline{\underline{\tau}}_G)\cdot\mathbf{n}]\cdot\mathbf{n} + p_G - p_L + \frac{1}{\mathrm{We}}\nabla\cdot\mathbf{n} - \frac{1}{\mathrm{Fr}}f = 0,$$

$$[(\underline{\underline{\tau}}_L - \underline{\underline{\tau}}_G)\cdot\mathbf{n}]\cdot\mathbf{t}_i = 0, \quad i = 1,2, \tag{1}$$

$$u_G = \sqrt{\rho_G/\rho_L}\,u_L,$$

where the subscripts L and G stand for liquid and gas, respectively, $\underline{\underline{\tau}}$ is the viscous stress tensor, f measures the vertical displacement of the interface with respect to the midplane, and $\mathbf{n}$ and $\mathbf{t}_i$ are the normal and the two tangential unit vectors, respectively. The Weber and Froude numbers are defined by

$$\mathrm{We} = \rho_L h u_{\star_L}^2/\sigma \quad \text{and} \quad \mathrm{Fr} = u_{\star_L}^2 \rho_L / gh(\rho_L - \rho_G), \tag{2}$$

respectively, where σ is the surface tension coefficient, were selected ($\mathrm{We}=4.8\times10^{-3}$ and $\mathrm{Fr}=8.7\times10^{-5}$) so as to limit the flow to the range of capillary-gravity waves.

Periodic boundary conditions were applied in the streamwise (x) and spanwise (y) directions. Turbulence generation is avoided at the outer boundaries by imposing free-slip conditions. The interface motion is computed by solving an advection equation for the vertical elevation of the interface, denoted by $f(\mathbf{x},t)$:

$$\partial_t f + \mathbf{u}\cdot\nabla f = 0. \tag{3}$$

This is known as the *boundary fitting* method,[16] since it relies on solving separately the two phases, and therefore cannot handle strong topological changes such as fragmentation and wave breaking. In this method, the distorted physical domain is mapped at each time step onto a rectangular parallelepiped on which the Navier-Stokes equations are solved using a pseudospectral technique.[3,16] The dimensions of the computational domain were $4\pi h\times 2\pi h\times 2h$ (with $h=0.02$ m), corresponding to $1074\times537\times171$ wall units in the streamwise, spanwise, and normal directions, respectively. A $64^2\times65$ resolution is used for the DNS against $32^2\times33$ for the LES. The density ratio between the two phases was $\rho_l/\rho_G=900$, corresponding to air-water flows at atmospheric pressure and at roughly 320 K. The liquid shear velocity $u_{\star_L}$ was set to 0.001 m/s. The usual 3/2 dealiasing rule systematically applied for both the DNS and LES. A statistical data analysis was accomplished by averaging the results over the two homogeneous directions ($x-y$ plane average), then over time.

III. LES OF TURBULENCE AT A DEFORMABLE GAS-LIQUID INTERFACE

A. The filtered equations

In the boundary fitting context where the phases are treated separately, the filtered mass and momentum equations for each phase are equivalent to the single-phase LES equations, which in Fourier-Chebychev space take the form

$$\mathbf{k}\cdot\mathbf{u}_\mathbf{k}^\mathbf{R} = 0, \tag{4}$$

$$\left(\frac{\partial}{\partial t} + \frac{1}{\mathrm{Re}\star}|\mathbf{k}|^2\right)\mathbf{u}_\mathbf{k}^\mathbf{R} = -i\mathbf{k}p_k^\mathbf{R} - i\mathbf{k}\cdot[(\mathbf{u}^\mathbf{R}\otimes\mathbf{u}^\mathbf{R})_\mathbf{k} + \mathbf{R}_\mathbf{k}], \tag{5}$$

where $\mathbf{u}_\mathbf{k}^\mathbf{R}$ is the resolved velocity vector, $p_\mathbf{k}^R$ is the resolved dynamic pressure, both obtained by filtering—using $G(\mathbf{k})$—the primitive flow field (e.g., $\mathbf{u}^\mathbf{R}(\mathbf{k},t)=G(\mathbf{k})\cdot\mathbf{u}(\mathbf{k},t)$), and $\mathbf{k}$ is the wavenumber vector. Quantities appearing with subscript $\mathbf{k}$ are coefficients in Fourier-Chebychev space. The unresolved SGS stresses to be modeled are defined by

$$\mathbf{R}_\mathbf{k} = (\mathbf{u}\otimes\mathbf{u})_\mathbf{k}^R - (\mathbf{u}^\mathbf{R}\otimes\mathbf{u}^\mathbf{R})_\mathbf{k}. \tag{6}$$

The above set of equations is solved in each domain using the proper material properties. The separate flow solutions are then coupled through the jump conditions, once the filtered interface topology equation is solved.

B. The projected equations in VMS

In contrast to space filtering described above, LES equations in VMS are derived by applying *a priori* scale separation to the primitive equations,[1] i.e., by projecting the exact solution on a smaller function space. This virtually avoids having to model the unresolved interfacial scales that appear in the filtered single-fluid equations,[7,17,18] which is the other key issue in the LES of this class of flow.

The solution space $\mathcal{V}$ is thus partitioned between large resolved scales, small resolved scales, and unresolved scales, respectively:

$$\mathcal{V} \equiv \mathcal{V}^R \oplus \mathcal{V}^{NR} = \hat{\mathcal{V}} \oplus \tilde{\mathcal{V}} \oplus \mathcal{V}^{NR}. \tag{7}$$

Flow variables are subsequently decomposed into their projections on each subspace:

$$\mathbf{u} = \underbrace{\mathbf{u}^\mathbf{R}}_{\text{Resolved field}} + \underbrace{\mathbf{u}^\mathbf{NR}}_{\text{Unresolved field}};$$

$$\mathbf{u}^\mathbf{R} = \underbrace{\hat{\mathbf{u}}}_{\text{Large scales}} + \underbrace{\tilde{\mathbf{u}}}_{\text{Small scales}}. \tag{8}$$

The mass and momentum equations governing the resolved scales of motions for incompressible flow of a Newtonian fluid are then written in Fourier-Chebychev space as two different sets of equations:

$$\mathbf{k}\cdot\widehat{\mathbf{u}_\mathbf{k}} = 0, \tag{9}$$

$$\left(\frac{\partial}{\partial t} + \frac{1}{\mathrm{Re}\star}|\mathbf{k}|^2\right)\widehat{\mathbf{u}_\mathbf{k}} = -i\mathbf{k}\widehat{p_k} - i\mathbf{k}\cdot[\widehat{(\mathbf{u}^\mathbf{R}\otimes\mathbf{u}^\mathbf{R})_\mathbf{k}} + \widehat{\mathbf{R}_\mathbf{k}}], \tag{10}$$

$$\mathbf{k}\cdot\widetilde{\mathbf{u}_\mathbf{k}} = 0, \tag{11}$$

$$\left(\frac{\partial}{\partial t} + \frac{1}{\mathrm{Re}\star}|\mathbf{k}|^2\right)\widetilde{\mathbf{u}_\mathbf{k}} = -i\mathbf{k}\widetilde{p_k} - i\mathbf{k}\cdot[\widetilde{(\mathbf{u}^\mathbf{R}\otimes\mathbf{u}^\mathbf{R})_\mathbf{k}} + \widetilde{\mathbf{R}_\mathbf{k}}]. \tag{12}$$

The effect of the unresolved scales appears through the SGS stress terms $\widehat{\mathbf{R}_\mathbf{k}}$ and $\widetilde{\mathbf{R}_\mathbf{k}}$ that should be modeled. The key point is that the two projections of the Reynolds stress play separate roles and can be modeled independently.

The above sets of equations are solved simultaneously for each phase using proper material properties. The separate flow solutions are then coupled through the jump conditions, once the interface topology equation is solved in the resolved space, $\mathcal{V}^R$:

$$\partial_t f^R + \mathbf{u}^\mathbf{R}\cdot\nabla f^R = 0. \tag{13}$$

The inspection of the wave saturation spectra of this flow (under the present physical conditions) provided by the DNS of Fulgosi *et al.*,[3] defined as

$$B(k) = k^2 2\pi^{-1}\int \overline{f(\mathbf{x},t_0)f(\mathbf{x}+\mathbf{r},t_0)}e^{-i\mathbf{k}\cdot\mathbf{r}}\,d\mathbf{r}, \tag{14}$$

reveals that high-wavenumber wave scales play a minor role in the range ($k_{\mathrm{LES}}<k<k_{\mathrm{DNS}}$), as compared to the velocity

field. The decay of wave saturation spectra reported in Ref. 3 $[B(k)\sim k^{-4}]$ is indeed faster than that of turbulence $(E_{kk}\sim k^{-5/3})$, for the same LES spectral cutoff k_{LES} for f and $\mathbf{u}$.

Unresolved interfacial scales are therefore less energetic than equivalent (in wavenumber) turbulence scales. This helps neglect the contribution from the unresolved/resolved turbulence/interfacial scales that should appear in Eq. (13), if the topology equation were to be treated in both $\mathcal{V}^R$ and $\mathcal{V}^{NR}$ subspaces, i.e., $\mathbf{u}^{\mathbf{NR}}\cdot\nabla f^R+\mathbf{u}^{\mathbf{R}}\cdot\nabla f^{NR}\approx 0$.

C. SGS and near interface modeling

1. The modified Smagorinsky model

In the presence of shear, be it near the wall or in the vicinity of sheared surfaces where the viscous sublayer is well resolved, SGS eddy viscosity models need, in general, to incorporate a damping function in order to accommodate the near-wall/interface limiting behavior. The DNS of countercurrent two-phase flow studies of Fulgosi *et al.*[3] have revealed the need for turbulence damping as the interface is approached, like in wall flows. A similar conclusion has been reached by Shen *et al.*[5] when exploring their DNS data of a free surface flow. A systematic LES study performed by Lakehal *et al.*[2] has shown that, without modification, the reference Smagorinsky model becomes excessively dissipative.

To summarize, the modified Smagorinsky model[2,7] employed in the filtered-equation LES context takes the form

$$\mathbf{R}=-2\nu_t\mathbf{S}(\mathbf{u}^R);\quad \nu_t=f_{\mu\mathrm{int}}(C_s\bar{\Delta})^2|\mathbf{S}(\mathbf{u}^R)|;$$
$$\mathbf{S}(\mathbf{u}^R)=\frac{1}{2}[\nabla\mathbf{u}^R+(\nabla\mathbf{u}^R)^T], \tag{15}$$

where $|\mathbf{S}(\mathbf{u}^R)|$ is the second invariant of $\mathbf{S}(\mathbf{u}^R)$, $f_{\mu\mathrm{int}}$ is the damping function inferred from the DNS data, $\bar{\Delta}$ is the cutoff filter width, and C_s is the Smagorinsky constant. Some empirical attempts were made to optimize the value of C_s and the best results overall were obtained for $C_s=0.1$, which coincides with the value used by Hughes *et al.*[1] in single-phase channel flow.

For low to moderate interface deformations, the DNS data of Fulgosi *et al.*[3] provides an exponential dependence of $f_{\mu\mathrm{int}}$ on the nondimensional distance to the interface y^+_{int} (referred to as "interface turbulence units") from the gas side:

$$f_{\mu\mathrm{int}}=1-\exp[-0.00013y^+_{\mathrm{int}}-0.00036(y^+)^2_{\mathrm{int}}-1.08E^{-05}(y^+)^3_{\mathrm{int}}]. \tag{16}$$

2. The variational multiscale approach

In applying the VMS methodology here, we have followed the strategy originally proposed by Hughes *et al.*,[1,9,10] in that truncation is used on a pseudospectral basis. This raises a couple of issues, in particular, the sensitivity of the approach to the nature of the scale separation operator employed. This has been addressed in this context, too, as it has been the case for single-phase flow.[10,12] The assessment approach used in Ref. 12 has been borrowed here for two different operators used to segregate large and small scales from the resolved field.

The first filter kernel for the secondary scale separation operator is the sharp spectral cutoff filter:

$$\hat{\mathbf{u}}(\mathbf{x},t)=\sum_{|\mathbf{k}|\leqslant k_c}\mathbf{u}_k(t)e^{i\mathbf{k}\cdot\mathbf{x}},\quad \tilde{\mathbf{u}}(\mathbf{x},t)=\sum_{k_c<|\mathbf{k}|\leqslant k'}\mathbf{u}_k(t)e^{i\mathbf{k}\cdot\mathbf{x}}, \tag{17}$$

where k_c stands for the cutoff wavenumber (now a modeling parameter). The optimal value of k_c lies around $k'/2$, where the wavenumber based on the grid resolution is $k'=2\pi/\Delta x$.

The second filter kernel employed is Gaussian:

$$\hat{\mathbf{u}}(\mathbf{k},t)=G(\mathbf{k})\cdot\mathbf{u}(\mathbf{k},t),$$
$$\tilde{\mathbf{u}}(\mathbf{k},t)=[1-G(\mathbf{k})]\cdot\mathbf{u}(\mathbf{k},t),\quad \forall\,|\mathbf{k}|\leqslant k', \tag{18}$$

with

$$G(\mathbf{k})=\exp\left(-\frac{\pi^2}{24}\frac{k^2}{k'^2}\right). \tag{19}$$

Note that here again, variables with subscript k implicitly refer to Fourier-Chebychev coefficients

For small scales, the SGS stress tensor is approximated using a Smagorinsky-type eddy viscosity model, without a damping function:

$$\tilde{\mathbf{R}}=-2\widetilde{\nu_t}\mathbf{S}(\tilde{\mathbf{u}});\quad \widetilde{\nu_t}=(C_s\hat{\Delta})^2|\mathbf{S}(\tilde{\mathbf{u}})|, \tag{20}$$

where $|\mathbf{S}(\tilde{\mathbf{u}})|$ is the second invariant of $\mathbf{S}(\tilde{\mathbf{u}})$. There the optimal value of the constant C_s clearly depends on the shape of the segregation filter (cf Sec. III D), albeit, as mentioned previously, the best fit was empirically found for $C_s=0.1$.

The projection of the subgrid stress tensor on the large scales subspace $\hat{\mathcal{V}}$ is taken to be equal to zero. Note that if the two subspaces $\tilde{\mathcal{V}}$ and $\hat{\mathcal{V}}$ were orthogonal, like in the case of the spectral cutoff filter, this choice implies that the subgrid dissipation for large scales is zero, and that the direct effects from the unresolved scales on large resolved scales can be neglected.

D. Sensitivity to scale partition

Sensitivity to scale partition in VMS for single-phase flows has been analyzed in Refs. 10 and 12. These studies show that the ratio of the large scales to the total resolved scales in each direction (k_c/k') and the filter kernel cannot be chosen independently. A sensitivity analysis has therefore been performed for this flow too, where a wide range of parameter variations was conducted. Only selected results obtained with the sharp cutoff filter are presented later.

As was to be expected from previous VMS simulations,[12] deviations from the DNS are model dependent, in that variations of selected parameters produce notable differences in averaged quantities. Among these parameters, there is the cutoff partition between large resolved scales and small resolved scales and the value of the C_s constant. This sensitivity is quantified through three test cases, corresponding to simulation runs with slightly different parameters (see Table I). To shed light on the coupling between the fluids, only one parameter is changed at the time and for only one phase.

TABLE I. VMS parameters used for comparison. Simulations with the sharp cutoff filter.

	Gas phase		Liquid phase	
Case	k_c/k'	C_s	k_c/k'	C_s
C1	0.5	0.1	0.5	0.15
C2	0.6	0.1	0.5	0.1
C3	0.5	0.1	0.5	0.1

Figure 1 compares cases C2 and C3, that differ only by the value of the cutoff filter scale ratio in the gas phase. It is clearly seen that the changes in the parametrization affects primarily the viscous sublayer. Spanwise and vertical components of velocity fluctuations in both phases experience very little variations, but more significant deviations are observed for the streamwise component, for which both rms and mean velocity (see Fig. 2) are affected. It is interesting to notice how the deviation in the gas alters the mean flow in the liquid very near the interface. We also note the strong sensitivity of the liquid, in general, to the change in parameters as compared to the gas phase, in particular, in the blockage layer where u' rms velocity is overpredicted.

Case C1 is identical to C3, except that C_s in the liquid is set equal to 0.15 instead of 0.1. Little difference is seen in the gas phase, but all high-order statistical moments in the liquid are affected. In fact, it could be that the simulation with C_s=0.1 in the liquid would have provided results less affected than with C=0.15. In particular, the pressure-strain correlation budget close to the interface is shifted toward a larger transfer of energy from the streamwise component to the vertical one [see Fig. 3(b)]. This issue will be discussed later on, when more detailed results are presented for the energy transfer and balance.

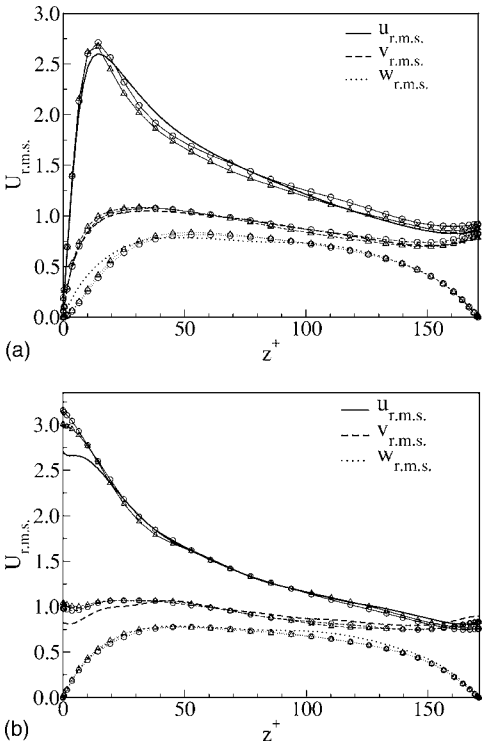

FIG. 1. Turbulence intensities on both sides. The quantities are normalized by the friction velocity. (Lines), DNS; (△), C2; (○), C3.

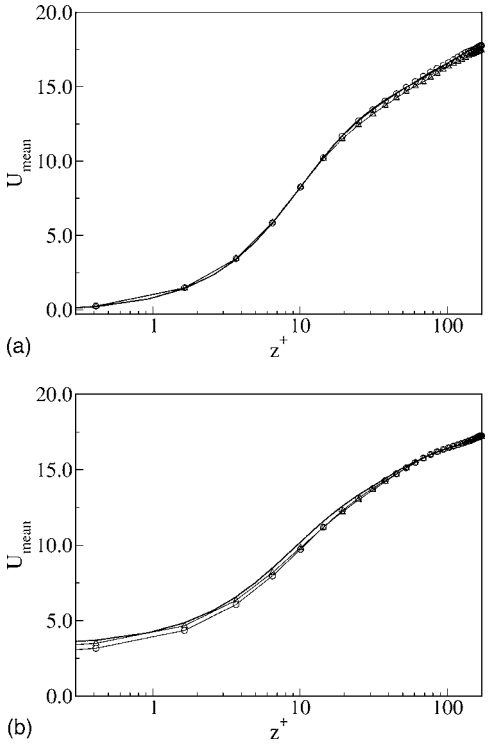

FIG. 2. Mean velocity profiles on both sides. The quantities are normalized by the friction velocity. (Lines), DNS; (△), C2; (○), C3.

According to Sagaut and Levasseur,[12] the sensitivity of the model should be less acute for the Gaussian filter as compared to the sharp cutoff filter. Direct effects of unresolved scales on the large physical scales of the flow are not

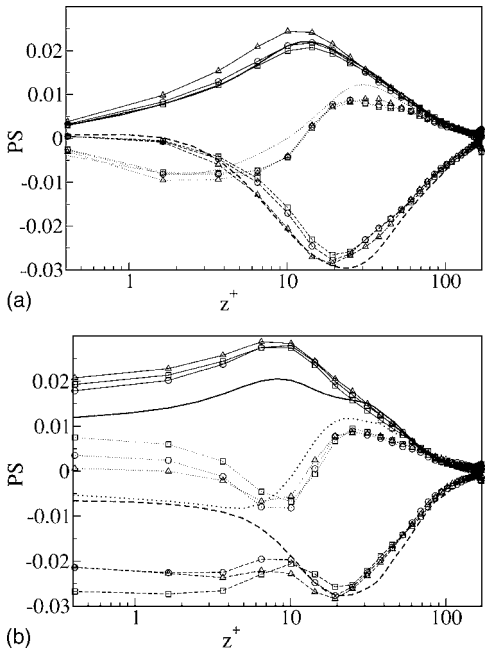

FIG. 3. Profiles of the pressure-strain correlations. (Lines), DNS; (□), C1; (△), C2; (○), C3. (—), PS_2; (---), PS_1 and (···) PS_3.

TABLE II. Errors in the mean and rms velocity fluctuations.

	Gas		Liquid		Gas		Liquid	
Case	U_{mean}	rms	U_{mean}	rms	k_c/k'	C_s	k_c/k'	C_s
C1	0.074	0.057	0.204	0.081	0.5	0.1	0.5	0.15
C2	0.320	0.089	0.150	0.096	0.6	0.1	0.5	0.1
C3	0.066	0.072	0.160	0.102	0.5	0.1	0.5	0.1
C4	0.219	0.065	0.100	0.084	0.5	0.12	0.5	0.12
C5	0.102	0.071	0.095	0.127	0.6	0.12	0.6	0.12
C6	0.890	0.230	0.210	0.260	0.4	0.16	0.4	0.16
C7GAUSS	0.183	0.059	0.13	0.103	0.64	0.2	0.64	0.2
C8GAUSS	0.241	0.074	0.139	0.132	0.45	0.1	0.45	0.1

neglected anymore since the SGS terms acting on small wavenumbers are no longer zero. Additional simulations based on the use of the Gaussian filter have been performed for different filter widths and the results compare in general to DNS,like with the spectral cutoff filter. Nevertheless, this sensitivity analysis with regard to scale partition is in fact very closely linked with the optimal choice of C_s. If indeed one tunes the ratio of small to large resolved scales (i.e., k_c/k' or the Gaussian filter width), then the total amount of SGS dissipation added by the multiscale model is also modified. As it should theoretically be adjusted to match the dissipation calculated from the DNS, i.e., the energy transfer from GS to SGS scales, the C_s constant of the model has to be modified. An ideal analysis of the sensitivity of the VMS to scales partition should therefore include optimization with respect to C_s. This can be done analytically in the case of the spectral cutoff filter,[12] but it is much more illusive (if ever possible) to derive an explicit correlation between C_s and the filter width in the Gaussian filtering in the general case. It is worth noting that other self-adaptive subgrid models based on the use of a test filter, such as dynamic models have also been found to be sensitive to the test filtering parameter.

Table II displays a measure of sensitivity for the mean and rms streamwise velocities for various combinations of the constant C_s and the ratio k_c/k'. The error for a variable ϕ is defined as an integral over the domain volume V:

$$\text{error}(\phi) = \frac{1}{V}\sqrt{\int_V (\phi - \phi_{\text{DNS}})^2\, dV}, \tag{21}$$

where ϕ_{DNS} denotes the exact DNS reference value. A close look at the results shows that the sensitivity exercise is complex, since a decrease in the error in the mean flow velocity in one phase has no direct repercussions on the other phase. In some cases, improvement in one phase results in an error increase in the second phase. The best parametrization is denoted in the table by C1 for the gas phase and C4 in the liquid, which differ by the values of C_s. Considering all the runs, it seems that the optimal parametrization for both phases when using the sharp cutoff filter is obtained for case C1 and C3, both using $k_c/k'=0.5$ and $C_s=0.1$ in the gas and $C_s=0.15$ and 0.1 in the liquid. We note additionally that the LES of the liquid flow is more sensitive to the value of the model constant C_s when using the sharp cutoff filter than to the Gaussian filter. The optimization of VMS-based models is therefore much more complex in interfacial and free-surface flows than in single-phase channel flow and boundary layers. The dynamics of the interface indeed plays an important role in redistributing turbulent stresses, and LES is necessarily associated with a smoothening of the interfacial topology that could play a role in these redistribution mechanisms.

E. *A priori* test

The *a priori* analysis performed here aims at elucidating the transfer mechanisms returned by each SGS model on both sides of the interface. A similar sensitivity analysis has been carried out in Ref. 19 for channel flow. The comparison includes the filtered DNS data. The SGS models were first applied to the filtered velocity field of the DNS; then the SGS dissipation was evaluated with the modeled stresses. The quantity of interest here is what we refer to as "SGS exchange," misleadingly known in the open literature as "SGS dissipation," since it governs both the top-down and bottom-up exchange of energy between GS and SGS turbulence [see also Eq. (24)]:

$$\varepsilon^{\text{SGS}} = \langle R_{kl} S^R_{kl} \rangle. \tag{22}$$

In the above expression, S^R_{kl} stands for the resolved rate of strain tensor. The averaging operator $\langle\ \rangle$ means that the data were first spanwise averaged then time averaged. Positive values of the SGS dissipation indicate a flux of kinetic energy from large to small scales, and negative values indicate a bottom-up backscatter of energy.

The results are shown in Fig. 4 for both the gas and liquid sides, along with the filtered DNS data. Panels (a) and (b) of the figure show that in all cases energy is flowing from large to small scales. The trend is well predicted by all the SGS models employed, although the values delivered by the Smagorinsky model alone are excessively higher than the DNS. This alone explains the counterperformance of the model in each phase; the values are actually one order of magnitude higher than the DNS. The behavior of the modified Smagorinsky model is remarkable on both sides of the interface, where it compares very well to the DNS. It returns, however, values close to zero at the interface, when seen from the liquid side, like in the air side. This is because the

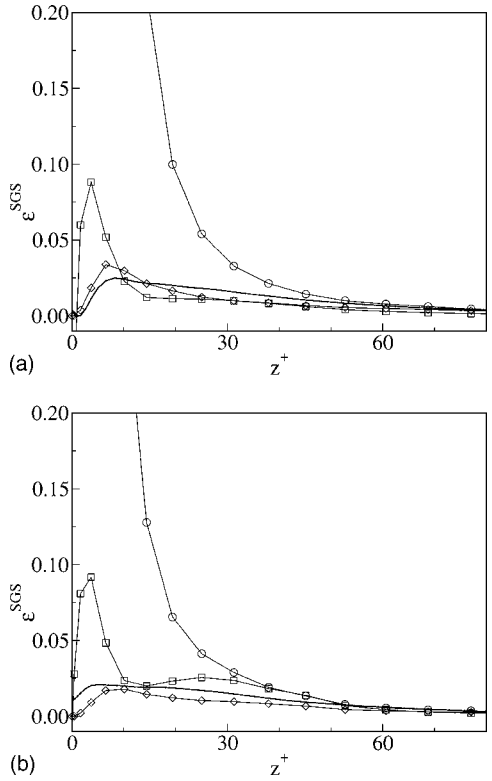

FIG. 4. SGS exchange ε^{SGS}. A comparison of DNS results with various SGS models: Lines, DNS; lines with symbols, LES. (○), LES with reference Smagorinsky model; (◇), LES with SGS and Eq. (16); and (□), VMS.

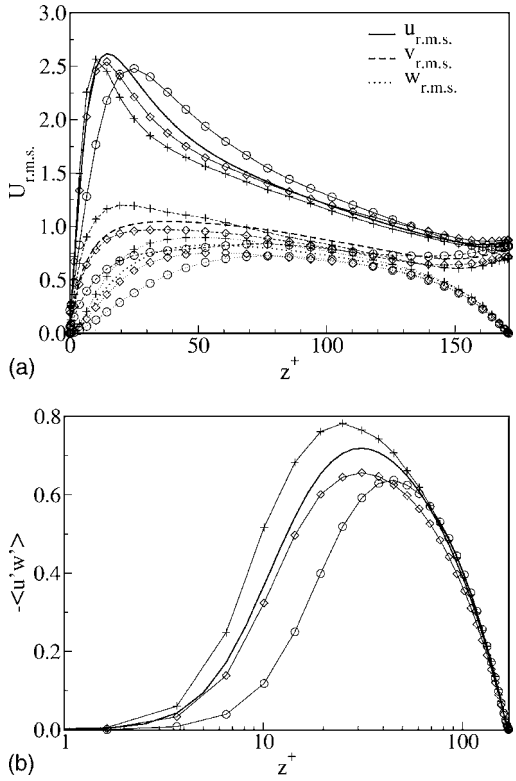

FIG. 5. Turbulence intensities and shear stress profiles in the gas phase: Lines without symbols, DNS; (+), under-resolved DNS; (○), LES with reference Smagorinsky model; (◇), LES with SGS and Eq. (16).

same damping function has been used for both phases, and this needs to be reexamined. The VMS somewhat overpredicts the dissipation in the viscosity-affected layer. But since the result has been obtained for a specific resolution, a specific cutoff filter, a specific set of values for C_s, with the assumption of orthogonality of the subspaces, a definitive conclusion can hardly been drawn in this regard. Another "setup" would provide another result, and that is why a unified LES strategy needs still to be defined within the VMS paradigm.

The excessive levels of the modeled dissipation ε^{SGS} overall degrade the LES results within the buffer layer, such as with the Smagorinsky model of reference, as shown above. However, it is really questionable that slight differences between the VMS and the modified Smagorinsky model can make such a strong difference in the averaged results. The reasons for the outperformance of the VMS are in its capacity to control the energy transfer in the spectral domain, where energy is extracted only from high wavenumber modes. The results obtained here rather mean that for the particular conditions used, the large-scale motions should indeed not be sensitive to eddy viscosity, otherwise the activity there would be exaggerated. As compared to the channel-flow DNS of Hartel and Kleiser,[19] the filtered DNS does not exhibit a long-range transfer of energy from the low wavenumber modes to the subgrid scales, which in this case relaxes the demands for the VMS. The filtered channel-flow data of Ref. 19 show indeed a backscatter of energy that we do not observe in the present results.

IV. *A POSTERIORI* RESULTS OF THE SMAGORINSKY SGS MODELS

The comparison between full DNS, under-resolved DNS, and selected LES results obtained with the reference and modified Smagorinsky models is discussed in Figs. 5 and 6 for the gas phase, where various key quantities are compared as a function of the distance to the interface. More detailed comparisons are available in Ref. 2. To summarize, the reference SGS model was shown to fail in reproducing the boundary layer characteristics. The mean velocity profile was grossly underpredicted as well as the turbulent shear stress [Fig. 5(b)]. Combining the SGS model with the near-interface damping function led to much better mean-flow results. The LES results (not included) in the liquid side were far off from the DNS data, probably because the eddy viscosity damping was not applied to the liquid side.

Turbulence intensities are plotted in Fig. 5(a) versus the nondimensional distance to the interface; the graph includes the results of the under-resolved DNS (32^3). It is clearly shown that without a SGS approximation the results deviate considerably from DNS. While the fluctuations are underestimated in the streamwise directions, they are grossly overestimated in the spanwise and vertical directions. The SGS model of reference is clearly dissipative, and this can be judged from the shift of the peak in turbulence intensity, which corroborates with the shift in the turbulent shear stress observed in the right panel of the figure. The turbulent shear stress plotted in Fig. 5(b) are correctly predicted by the model with the damping function. Overall, introducing the

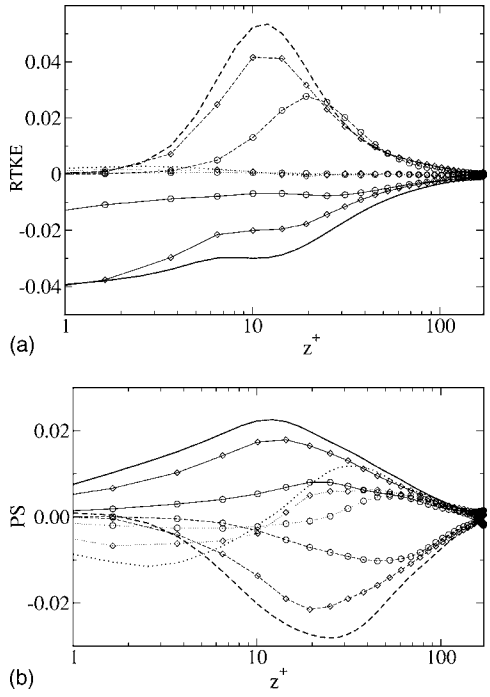

FIG. 6. Terms in the budget for the resolved kinetic energy RTKE, $K=\langle u_k' u_k' \rangle/2$ (a). Lines, DNS; lines with symbols, LES. (—), Gain; (---), loss. (○), LES with reference Smagorinsky model; (◇) LES with SGS and Eq. (16). Profiles of pressure-strain correlations (b). (—), PS_2; (---), PS_1, and (···) PS_3.

near-interface treatment via Eq. (16) has been found to considerably enhance the quality of the results. Hughes *et al.*[1] observed the same model behavior for channel flow simulation. In both the panels, the under-resolved DNS data do not match the DNS and indicate the need for modeling the effect of under-resolved scales.

A higher-order analysis of the results centers on the energy transfer mechanisms obtained by analyzing the kinetic energy of the resolved (GS) motions, and the pressure-strain correlations defined next. The resolved kinetic energy $E^R \equiv u_k^R u_k^R/2$ reads as

$$\frac{\partial E^R}{\partial t} + \frac{\partial u_j^R E^R}{\partial x_j} = -\frac{\partial p^R u_i^R}{\partial x_i} + \frac{1}{\mathrm{Re}^*}\frac{\partial^2 E^R}{\partial x_j^2} - \frac{1}{\mathrm{Re}^*}\left(\frac{\partial u_i^R}{\partial x_j}\right)^2 + R_{ij}\frac{\partial u_i^R}{\partial x_j} - \frac{\partial}{\partial x_j}(R_{ij}u_i^R), \tag{23}$$

where the last two terms in the right-hand side denote the SGS interaction effects with the resolved field consequent to filtering or projection of the primitive DNS equations. A detailed meaning of each component will follow from the balance presented later. A statistical analysis of the balance requires first the definition of the statistical averaged kinetic energy equation, i.e., $\langle E^R \rangle \equiv \langle u_k^R u_k^R \rangle/2$; the averaged difference between the two quantities should represent precisely the balance to be compared later. Note that $\langle E^R \rangle$ can only be derived from the statistical averaged momentum equation. The statistical averaging performed amounts to splitting any resolved quantity g^R into its statistical mean and a fluctuation,[19] including the SGS stress R_{ij}, i.e., $g^R = \langle g \rangle + g'$.

The balance for the resolved turbulent kinetic energy (RTKE), $K=\langle u_k' u_k' \rangle/2$, therefore takes the form

$$\frac{DK}{Dt} = \underbrace{-\langle u_i' u_j' \rangle \frac{\partial \langle u_i^R \rangle}{\partial x_j}}_{\text{Prod.}} \underbrace{-\frac{\partial \langle p' u_i' \rangle}{\partial x_i}}_{\text{Press. Diff.}} \underbrace{-\frac{\partial \langle u_i' u_i' u_j' \rangle}{\partial x_j}}_{\text{Turb. Transp.}} + \underbrace{\frac{1}{\mathrm{Re}^*}\frac{\partial \langle u_i' u_i' \rangle^2}{\partial x_j^2}}_{\text{Visc. Diff.}} \underbrace{-\frac{1}{\mathrm{Re}^*}\left(\frac{\partial \langle u_i' \rangle}{\partial x_j}\right)^2}_{\text{Dissip.}} + \underbrace{\left\langle R_{ij}' \frac{\partial u_i'}{\partial x_j} \right\rangle}_{\varepsilon^{\mathrm{SGS}}} \underbrace{-\frac{\partial}{\partial x_j}\langle R_{ij}' u_i' \rangle}_{\mathcal{T}^{\mathrm{SGS}}} = 0, \tag{24}$$

where SGS exchange and SGS transport terms are denoted by $\varepsilon^{\mathrm{SGS}}$ and $\mathcal{T}^{\mathrm{SGS}}$, respectively; the sum will be denoted by E^{SGS}. Panel (a) of Fig. 6 compares the most relevant statistically averaged terms on the right-hand side of Eq. (24), namely, the GS production, the GS viscous dissipation, and the GS pressure diffusion; the SGS contributions will be treated in the corresponding section. Significant differences can be observed close to the interface. In all the LES simulations, the dissipation rate close to the interface was found to balance entirely the viscous diffusion, exactly as in the DNS of this flow and of similar wall flows. The production and dissipation terms are underestimated by the reference SGS model, resulting in near-interface asymptotic behaviors well below the DNS. The correction brought by the damping function substantially improves the energy budget, especially in the viscosity-affected region, $z^+ < 20$. The considerable underpredicted levels of production and dissipation returned by the SGS model of reference are in line with the mean velocity and shear stress distributions.

The manipulation of the averaged GS pressure diffusion term permits to extract the pressure-strain correlations (PS), defined by

$$\mathrm{PS}_i = \left\langle p' \frac{\partial u_i'}{\partial x_i} \right\rangle; \quad i = 1,2,3. \tag{25}$$

A positive value of PS_i implies a transfer of energy to component i from the other components, and vice versa. The sum of all the terms PS_i must converge toward zero by virtue of continuity.

Panel (b) of Fig. 6 compares the LES and DNS results of PS terms. The streamwise component (PS_1) transfers energy into the spanwise (PS_2) and the normal (PS_3) components. The redistribution between the terms is significantly dependent on SGS modeling. More than all the other terms, the comparison of the pressure-strain correlations clearly reveals the crucial need for near-interface damping to limit the dissipative behavior of the model. Results of the reference SGS model without modifications show very large deviations between LES and DNS data.

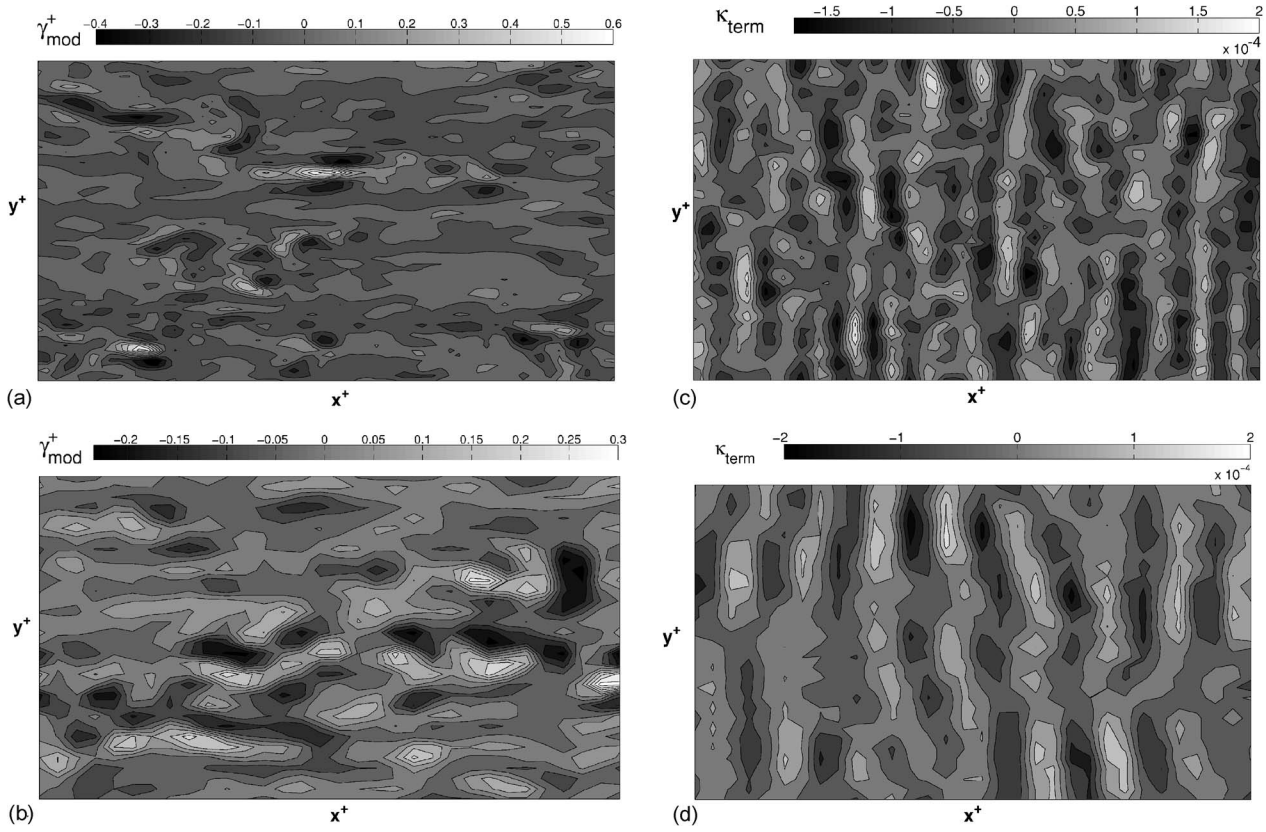

FIG. 7. Interfacial surface divergence term and surface dilation contribution.

V. *A POSTERIORI* RESULTS OF THE VMS APPROACH

The results analyzed below were obtained using $k_c/k'=0.5$, in connection with the spectral cutoff filter for both phases, but with $C_s=0.1$ in the gas and $C_s=0.15$ in the liquid. According to Table II, this combination yields the best results for each phase separately. In what follows, the primed quantities g' are defined from a statistical averaging sense, in that they represent the difference between the resolved field and its statistical average (over the homogeneous direction and over time): $g'=g^R-\langle g\rangle$.

A. Interfacial transfer

Close to gas-liquid interfaces,[20] surface divergence theory applies, meaning that

$$\gamma^+ = \left.\frac{\partial u'}{\partial x}+\frac{\partial v'}{\partial y}\right|_{\text{int}} = -\left.\frac{\partial w'}{\partial z}\right|_{\text{int}}$$

is finite because of surface renewal by upwelling eddies impinging at the surface in a random way. For rigid surfaces, $\partial w'/\partial z|_{\text{int}}$ should obviously converge toward zero. This vertical transport of fluid toward the surface and resulting mass transfer can therefore be quantified by γ^+, which should provide a faithful picture of the surface bursting motion. Figures 7(a) and 7(b) compare the DNS and LES data for γ^+. The comparison indicates that the VMS is capable to predict the most important bursting motions on the surface. The VMS results lie within the DNS interval, but as expected from a LES computation, small scales of the interface have been filtered out. What is expected indeed from LES is of course not to reproduce all the surface scales, but the most important bursting motions from the water, and that is successfully predicted by the VMS.

The vertical transport toward the surface by upwelling eddies is reflected by nonzero $w'|_{\text{int}}$ values and its gradient in the normal direction $\partial w'/\partial z|_{\text{int}}$, which actually plays the role of surface mass source. The stronger (or more frequent) the impingement of turbulent eddies toward the surface, the stronger the w' and interfacial deformations. This can be explained by examining the so-called *surface dilation* measure,[20]

$$\kappa_{\text{term}} = \frac{\partial w'}{\partial z} \sim -2w'\,\nabla\cdot\mathbf{n},$$

where $\mathbf{n}$ is the normal to the interface and $\nabla\cdot\mathbf{n}=\kappa$ its curvature. The results are plotted in Figs. 7(c) and 7(d). The above expression arises in a straightforward way by noting that in contrast to rigid walls, at a free surface the velocity fluctuations normal to the interface scales as $w'\propto w'_{,z}|_{\text{int}}z$, as a result of the boundary conditions, whereas at rigid surfaces it scales as $w'\propto w'_{,zz}|_{\text{wall}}z^2/2$. The dilation term is clearly shown to highlight the crests and the troughs marked by positive and negative isocontours, meaning that the interface deformations are well resolved by the LES. The wavelengths are also clearly visible from the figure. The LES results compare well with the DNS in terms of magnitude, but the DNS provides indeed a surface flow field dominated by numerous local regions of surface divergence. SGS models are indeed not

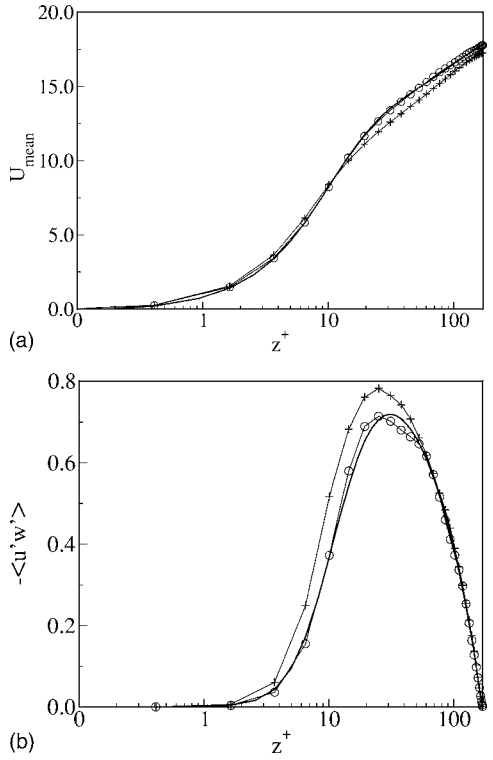

FIG. 8. Gas side—Comparison of mean velocity (a) and shear stress profiles (b) in wall coordinates: Lines, DNS; (+), under-resolved DNS; (○), VMS.

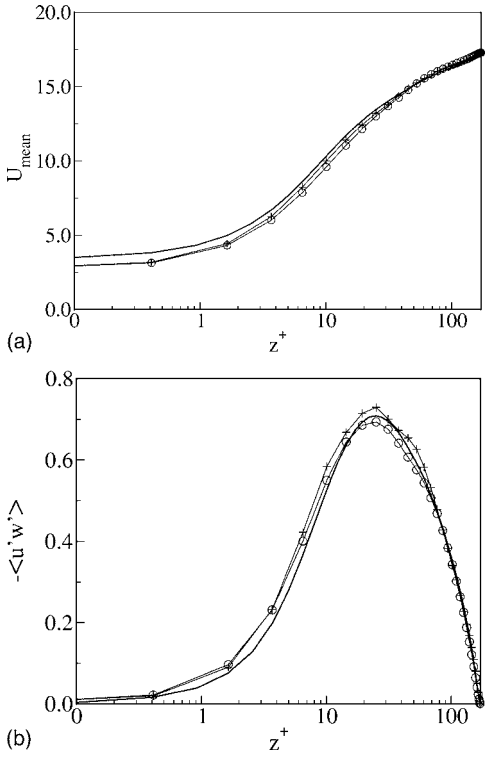

FIG. 9. Liquid side—Comparison of mean velocity (a) and shear stress profiles (b) in wall coordinates: Lines, DNS; (+), under-resolved DNS; (○), VMS.

expected to reproduce these flow details, but rather help prevent their dissipation.

B. Mean and rms profiles

Details of the comparison with full and under-resolved DNS data are displayed in Figs. 8 and 9, where the mean streamwise velocity and shear stress profiles in gas and liquid are compared as a function of the nondimensional distance to the interface. Note that the same computational and physical parameters were employed for the VMS and earlier LES simulations presented in the previous section. On the gas side the velocity profile and the shear stress distribution are remarkably well predicted. In the liquid the mean velocity is underestimated within 9% error close to the interface and within 1% error in the bulk. The trend of the turbulent shear stress is correctly predicted by the model, albeit it is slightly overestimated near the interface in the liquid side. The under-resolved DNS data deviate significantly from the DNS; the LES results are better.

The velocity fluctuations in the three directions are plotted versus the nondimensional distance to the interface in Fig. 10. The LES results compare very well with the DNS, except for the peak of turbulence intensity in the gas and the near-interface turbulence intensities in the liquid that are somewhat overestimated. Turbulence activity near the interface is more sustained in the liquid side than in the gas side, with a higher degree of anisotropy (two-component turbulence). While the vertical fluctuating velocity component decreases due to gravity and surface tension, the streamwise and lateral components are promoted while approaching the surface from the liquid side. Dictated by the return-to-

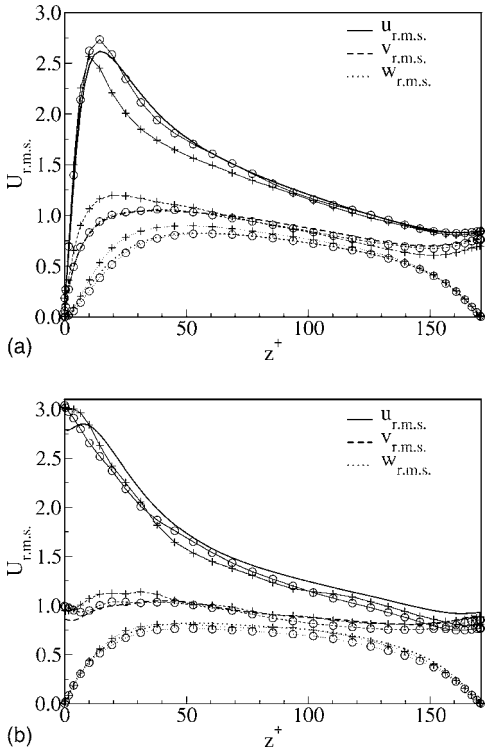

FIG. 10. Turbulence intensities in both phases. Lines, DNS; (+), under-resolved DNS; (○), VMS. Line styles are used to identify the different velocity components.

isotropy principle, the leading energy component u' extracts energy from the mean shear flow, and tends to redistribute it to the other components. This will be discussed in details when comparing pressure-strain terms. Apart from the slightly overestimated values in the viscous sublayer, the intercomponent redistribution mechanism within the fluctuating field is well reproduced by the VMS model.

The reference Smagorinsky model results in general in a shift of the peak of streamwise fluctuations and of the shear stress, as observed in the previous section. When applied within the multiscale framework, the overdissipative behavior of the model is compensated, which considerably enhances the quality of the results. As the interface is approached from the liquid side, however, the u' rms can be seen to be overestimated by the VMS, whereas the DNS indicates that this quantity in particular reduces abruptly there. This will have some consequences on the dissipation and pressure strain, as we shall see in the corresponding section. Note too that the increase of w' rms as the interface is approached in the liquid is well reproduced by the LES, better than in the gas side. Note finally that the under-resolved DNS data in the liquid are somewhat closer to the LES than is the case in the air side, in particular, for u' and w', but v' is overestimated near the interface. These are first-order statistics; the conclusion can be drawn only by inspecting higher-order moments results.

C. Turbulent kinetic energy budget

Additional understanding of the flow physics can be achieved through the analysis of the energy transfer mechanisms. The analysis starts by looking at the contribution of each term in the resolved turbulent kinetic energy balance (RTKE) defined previously by Eq. (24).

Figure 11 compares the most important statistically averaged terms on the right-hand side of Eq. (24), i.e., namely the production, the viscous dissipation, and the pressure diffusion of the GS motions; the SGS contributions will again be treated separately. We first note that, unlike in the gas side, where the shear-induced production goes to zero when the interface is approached, this quantity remains finite (though very small and constant in the range $0<z^+<0.1$) from the liquid side, because of the interfacial shear and normal $\bar{u}$-velocity gradient are finite, too.

Here again, no significant differences can be observed close to the interface. In all the LES simulations the dissipation rate close to the interface was found to balance entirely the viscous diffusion (results not shown), exactly as in the DNS of this flow and similar wall flows. For comparison, the production and dissipation were underestimated with the reference Smagorinsky model by 50% (Fig. 6). The improvement brought by the use of the multiscale approach is remarkable, especially in the viscosity-affected region, at $z^+<15$. The results obtained in the gas side are better than in the liquid side, in particular, the production. This result corroborates with the previous results of the mean velocity and shear stress obtained on both sides of the interface. It is important to note is that vìs-a-vìs the simulations with the modified Smagorinsky model [Eq. (16)], the VMS results are

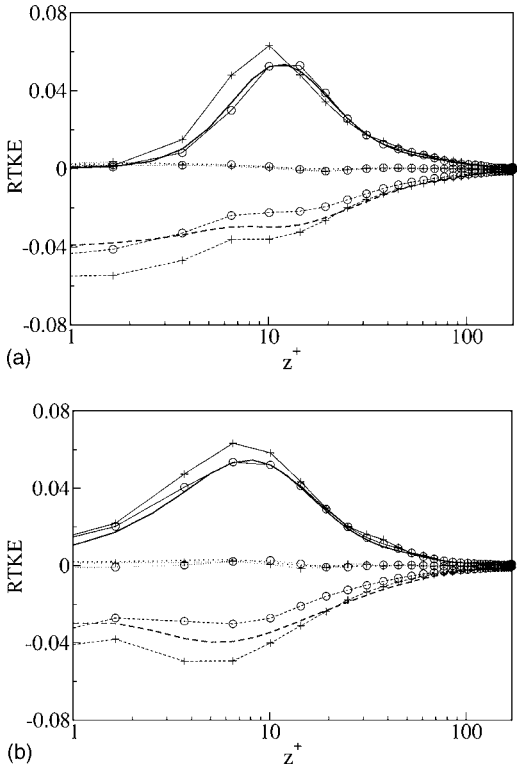

FIG. 11. Terms in the budget for resolved kinetic energy RTKE, $K=\langle u_k' u_k' \rangle/2$. Lines, DNS; (+), under-resolved DNS; (○), VMS. Line styles are used to identify the different terms: (—), production; (---) dissipation, and (···) pressure diffusion.

in excellent agreement with the DNS. The VMS results are therefore very interesting, and contribute to validating the model for the class of sheared interfacial flows studied here, i.e. gravity-capillary waves, without surface breaking.

The molecular dissipation is more sensitive to grid resolution since it directly involves the rms of the fluctuating field. Although slightly underestimated in the viscosity-affected regions, where the slopes of the normal streamwise velocity gradient deviate from the DNS data [Fig. 10(b)], the VMS results are still better than the data shown in Fig. 6; the model helps indeed recover most of energy dissipation rate lost by under-resolving the flow (32^3 DNS without a SGS model), at least in the gas side. On both sides of the interface, the under-resolved DNS data underpredict both the production and dissipation of turbulence. The conclusion is therefore clear: SGS modeling is necessary for the liquid phase (free-surface type of flow) as much as for the gas phase (wall type of flow).

D. Reynolds stress budget

The balance equation for the resolved normal stresses is similar to the resolved kinetic energy equation (RTKE), namely (for $k=1,2,3$),

$$\frac{D\langle u_k' u_k' \rangle}{Dt} = \mathcal{P} + \mathcal{T} + \Pi + \mathcal{D} - \varepsilon + \mathcal{T}_{kk}^{\mathrm{SGS}} + \varepsilon_{kk}^{\mathrm{SGS}} = 0; \qquad (26)$$

where $\mathcal{P}$ is the GS production, $\mathcal{T}$ is the resolved turbulent transport, Π is the pressure diffusion, $\mathcal{D}$ is the viscous diffu-

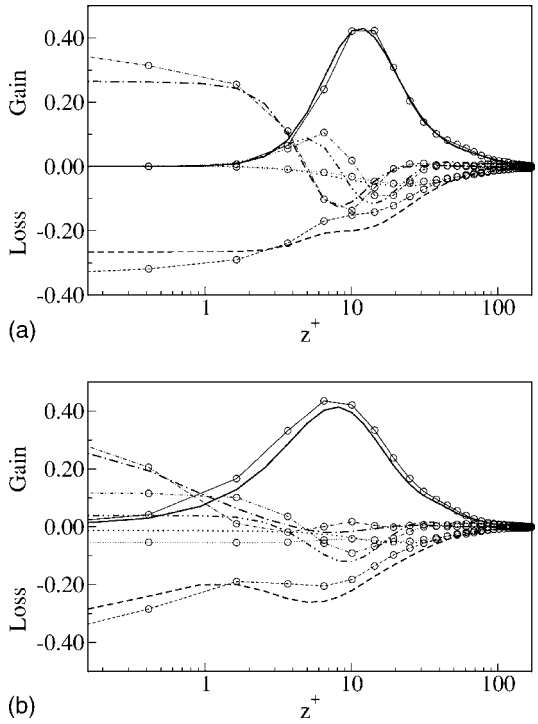

FIG. 12. Terms in the budget for $\langle u'u' \rangle$ in wall units. Lines, DNS; lines with symbols, VMS. (—), Production; (---) dissipation; (···), pressure diffusion; (-·-), viscous diffusion and (-···-), turbulent diffusion.

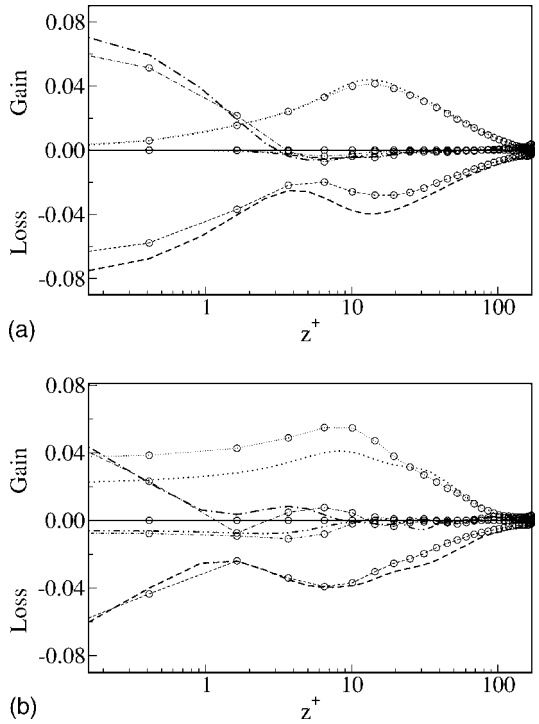

FIG. 13. Terms in the budget for $\langle v'v' \rangle$. Style definitions like in Fig. 12.

sion, ε is the molecular dissipation, $\mathcal{T}_{kk}^{\mathrm{SGS}} \equiv \langle (R'_{ij}u'_i)_j \rangle$ is the turbulent transport by SGS motion, and $\varepsilon_{kk}^{\mathrm{SGS}} \equiv \langle 2R'_{ij}u'_{i,j} \rangle$ reflects the SGS exchange mechanism. The sum of these two terms will be denoted by E_{11}^{SGS} and E_{22}^{SGS} for the first two components.

The pressure diffusion provides both a source and a redistribution mechanism of energy. It has been shown in the past[4,5] that the transfer of energy near unsheared free surfaces differs from the structure near rigid walls. It is therefore interesting to see with the present DNS whether the redistribution mechanisms are different for sheared, deformable interfaces, and whether this intercomponent transfer is within reach of LES, and how this is predicted by the SGS models employed.

We first compare the budgets of the resolved normal stresses. The comparison of the component $\langle u'u' \rangle$ is presented in Fig. 12 for both phases. Some discrepancies between the DNS and LES are observed in the vicinity of the interface ($z^+ < 10$). The values indicate that it is the streamwise stress that contributes most to the energy balance. Like in the resolved kinetic energy budget, the shear production is well predicted by the LES in the gas phase, and slightly underestimated in the liquid. As the interface is approached, the production decreases and the dissipation is entirely balanced by the viscous diffusion, which are both underestimated in the vicinity of the interface ($z^+ < 10$). This is mainly due to the turbulent shear stress reducing, because w' is reduced—albeit without converging to zero as in free surface flows where a zero-stress condition is imposed. Turbulent transport and pressure diffusion results compare well. In the liquid side, like for the resolved kinetic energy budget, the production is overestimated by the VMS. In contrast to the gas side, the energy balance in the liquid is somewhat different in the viscous sublayer, in that the dissipation is strong and is balanced not only by the viscous diffusion, but by the shear production and turbulent transport. All the terms become important in the liquid viscous sublayer. Here also the agreement between LES and DNS is remarkable, although the turbulent transport in particular is overpredicted.

The budgets for $\langle v'v' \rangle$ are presented in Fig. 13. Again, viscous diffusion and dissipation are of the same order of magnitude in the gas viscous sublayer, whereas turbulent transport is negligible and pressure diffusion decays as the interface is approached. The limits of the blocking layer are well marked by the importance of viscous mechanisms. In the spanwise direction there is no shear-induced production because the flow is fully developed. Very close to the interface the balance between dissipation and turbulent transport dominate the budget, whereas up to $z^+ > 10$ the dissipation is balanced by pressure diffusion. Apart from the dissipation, overall the LES results deviate very slightly from DNS. The pressure diffusion term, which in contrast to the gas side is finite in the liquid phase (energy absorber) is overpredicted by the VMS. The pressure diffusion term is overpredicted as well, whereas the dissipation is better predicted as compared to the gas side. Apart from that, we note that the structure of the energy distribution in the liquid is overall well predicted by the VMS.

Note that the DNS of Fulgosi *et al.*[3] has shown no substantial differences between the budget of all the Reynolds stress components in channel and sheared interfacial flow near the interface, but rather in the buffer region, $20 < z^+ < 40$, where pressure diffusion, turbulent transport, and dissipation were seen to be more pronounced by the waves.

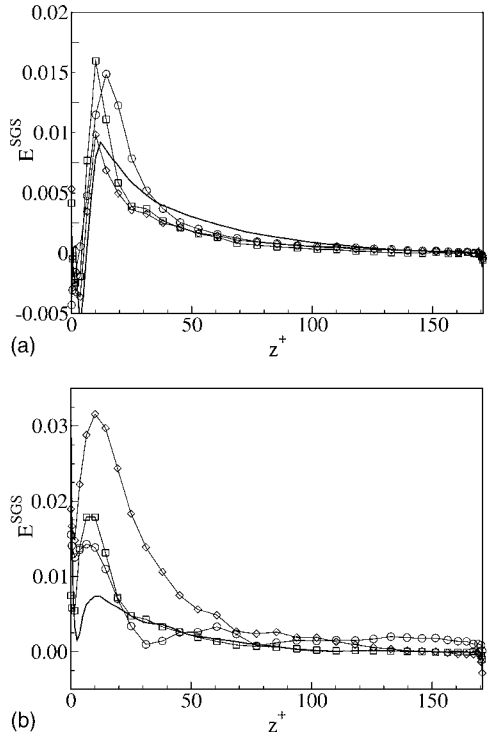

FIG. 14. SGS transport and exchange term E^{SGS} in the resolved kinetic energy balance equation. Lines, filtered DNS; lines with symbols, LES. (○), LES with reference Smagorinsky model; (◇), LES with SGS and Eq. (16); and (□), VMS.

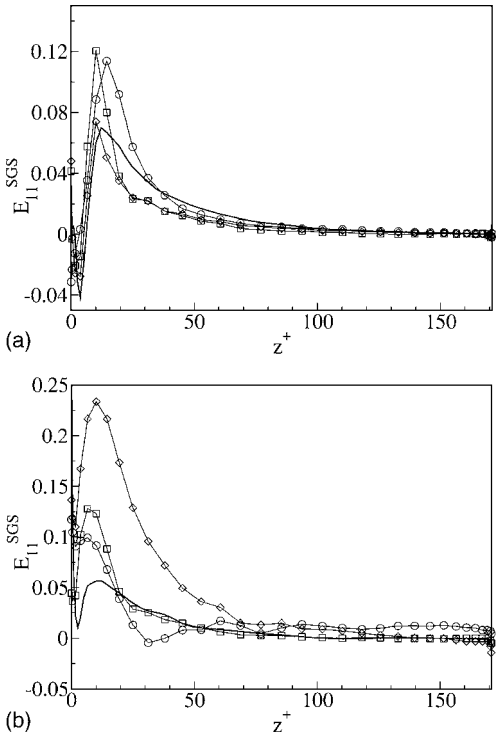

FIG. 15. SGS transport and exchange term E_{11}^{SGS} in the resolved streamwise normal stress balance equation. Lines, filtered DNS; lines with symbols, LES. (○), LES with reference Smagorinsky model; (◇), LES with SGS and Eq. (16); and (□), VMS.

E. SGS transport and exchange

In this section we focus on the SGS transport and exchange delivered by the SGS models employed, i.e., $E^{\mathrm{SGS}}=\langle \mathcal{T}^{\mathrm{SGS}}\rangle+\langle \varepsilon^{\mathrm{SGS}}\rangle$. The data are compared to the filtered DNS results. The total SGS contributions to the turbulent resolved kinetic energy defined above are compared in Fig. 14. In reality, the dominance of the SGS transport over the SGS exchange or vice versa depends primarily on how "precise" are the modeled SGS stresses, $\hat{R}_{ij}$ and $\tilde{R}_{ij}$. In the air side, the reference Smagorinsky model overpredicts the quantity up to $z^+=5$. Its modified variant applied in this phase only undepredicts the SGS transport and dissipation in the buffer layer, and overpredicts the peak value. The VMS results are consistent with the previous *a priori* results, in that it overestimates the level as compared to DNS. The VMS behaves somewhat better in the viscosity-affected layer. In the liquid side, all the SGS models employed overpredict the SGS transport and dissipation in the buffer layer. Surprisingly, it is the modified variant of the Smagorinsky model (applied in the gas phase only) that is the most dissipative in this case, in total odds with the previous *a priori* results of the SGS dissipation alone. This simply means that a similar damping of the eddy viscosity employed in the air side is also necessary for the liquid phase. The discrepancy results essentially from the SGS turbulent transport term, more exactly from the gradients of the SGS stresses. Note, finally, that the VMS results on both phases corroborate perfectly with the DNS from $z^+\approx 20$ and above. This demonstrates the ability of the model to select the scales on which R_{ij} is effective; in this case the activity of SGS turbulence is clearly negligible in the core flow region, where $z^+>20$, a feature within reach of the VMS only. Results (not included) with $Cs=0.1$ (C3) in the liquid rather than 0.15 may have been better since the SGS effects in the liquid are too high near the interface. But again, one can judge from these simulations that the VMS behaves in general well without too much manipulation of the model constants.

The SGS transport and exchange in the normal stress balance equations is plotted in Figs. 15 and 16. The analysis of the streamwise normal stress plotted in Fig. 15 is identical to the resolved kinetic energy: none of the SGS models is capable to correctly mimic the subtle mechanism of SGS transfer close to the interface, apart from the VMS, which behaves very well in both core flow regions, where z^+ is larger than 20.

Scrutinizing the liquid side results reveals once more the need for a near-interface damping in the liquid phase. The comparison of the SGS contributions in the resolved spanwise stress balance (E_{22}^{SGS}) in Fig. 16 reveals the difficulty for the SGS models to correctly mimic the transfer features. The VMS is shown to behave well in the liquid core flow, where the turbulence activity is selectively insensitive to the eddy viscosity.

F. Pressure-strain correlations

The last comparison between DNS and LES data concerns the pressure-strain correlations defined previously. Figure 17 shows the profiles of the pressure-strain correlation for both gas and liquid flows. The DNS results show that the

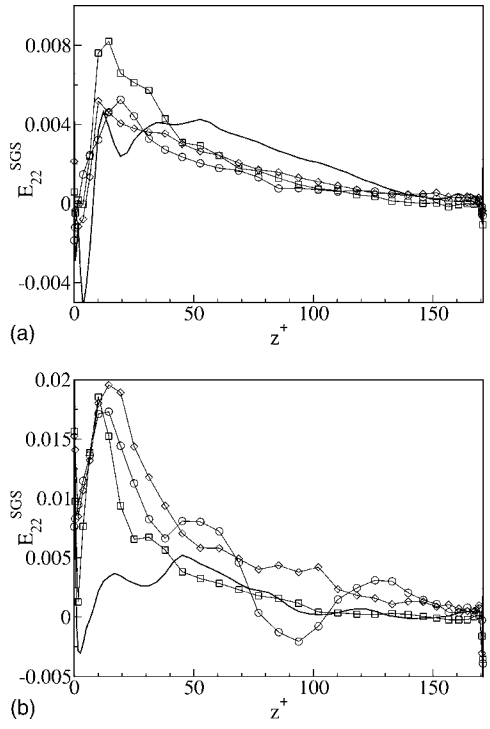

FIG. 16. SGS transport and exchange term E_{22}^{SGS} in the resolved streamwise normal stress balance equation. Line style definitions are like in Fig. 15.

streamwise component (PS_1) in the gas phase transfers energy into the spanwise (PS_2) and the normal (PS_3) components. The redistribution of energy has already been seen to be highly dependent on SGS modeling.[2] The results show that in the gas phase the scale separation successfully replaces near-interface damping: the VMS simulations predict indeed the right trend. The spanwise component is correctly predicted, whereas the energy transfers between streamwise and normal directions are slightly underpredicted.

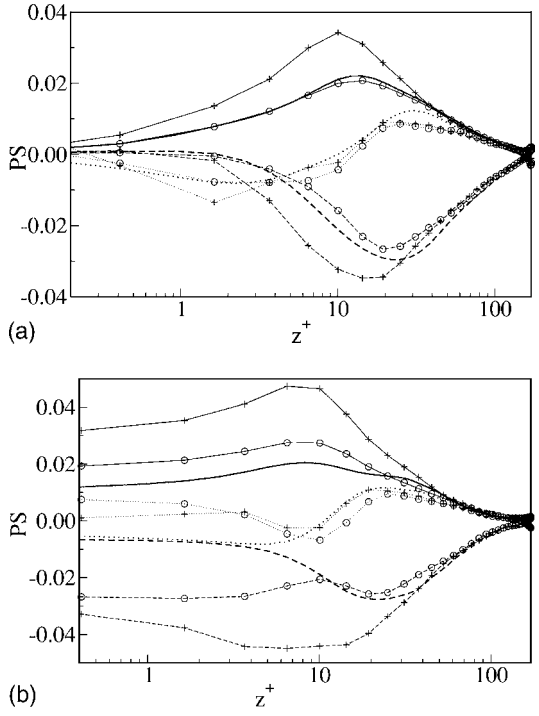

FIG. 17. Profiles of the pressure-strain correlation. Lines, DNS; (+), under-resolved DNS; (○), VMS. Line styles are used to identify the different terms: (—), PS_2; (---), PS_1, and (···) PS_3.

Figure 17(b) reveals that the energy transfer between the three directional components in the liquid side is not correctly captured in the near-interface blocking region ($z^+ < 10$). In the farfield, PS_2 and PS_3 are positive, whereas PS_1 is negative, and thus u' releases energy to v' and w'. This is well predicted by the LES. In the viscosity-affected layer where dissipation/diffusion balance dominate, the vertical component PS_3 changes sign and therefore w' loses energy to u' and v'. This is the signature of splat mechanisms or upwellings from the liquid core flow to the interface.[4] Here the LES fails to reproduce the sudden change in the intercomponent energy transfer. And by virtue of continuity, a deviation in one term should return deviations in the other two terms. One expects indeed from the DNS that the streamwise and vertical component equally contribute to transfer energy into the spanwise component. This deviation is restricted to the blocking region close to the interface but it may explain the slight underprediction of the mean velocity throughout the liquid (Fig. 9). The under-resolved DNS data are deviate significantly from both the DNS and LES.

Whether the deviations between LES and DNS results are solely due to $\langle \partial u_k'/\partial x_k \rangle$ itself or its rms is unclear; pressure fluctuations at the interface are extremely sensitive to model dissipation, and could therefore be implicated since they enter the definition of the pressure strain. In nondissipative SGS or under-resolved DNS simulations, a higher rms of p' indicate that high-wavenumber structures are not dissipated, but rather pile up at the upper end of the spectra. This should be felt by the pressure since it strongly interact with the fluctuating velocity field, as clearly shown in Fig. 18. The plots show indeed that the rms of p' for both phases is very high for under-resolved DNS, and the LES is capable to restore a non-negligible part of it. Clearly, the prediction of the fluctuating pressure in the viscosity-affected layer is the key to the energy transfer mechanism.

VI. CONCLUSIONS

In this study we aim at paving the way for future use of LES for turbulent interfacial flows. The base test case selected for validation here involves a the flow over a deformable, sheared interface, in which turbulence is generated at the interface due to the nonslip motion of the lighter phase over the heavier one. The reference Smagorinsky model has been applied with and without a near-interface damping DNS-based function. The core model was then used in combination with a multiscale VMS-based approach, in which a segregation into large and small portions among resolved scales is assumed *ab initio* with a selected scale-separation ratio. To the knowledge of the authors, this is the first application of the variational multiscale method to a two-phase flow. An *a priori* analysis has shed light on the performance of all the approaches in both fluid flows. Data have then been analyzed (*a posteriori*) in both the gas and the liquid, and

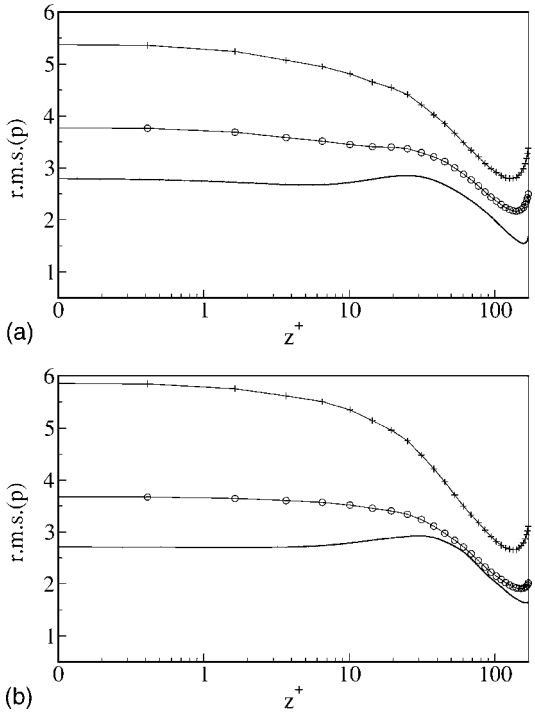

FIG. 18. Profiles of the pressure fluctuations. Lines, DNS; (+), underresolved DNS; (○), VMS.

compared to existing DNS data obtained using the same pseudospectral solver, for the same physical and computational parameters. The VMS approach was shown to be potentially promising for tackling interfacial flows, and is clearly best suited for a range of similar problems in which immiscible sheared phases are in direct contact. The approach is revealed to be quite sensitive to filter scale partition, in particular, in the higher density fluid. The optimum calibration of the VMS was obtained for a scale partition of $k_c/k' = 0.5$, and $C_s = 0.1$ in the gas side, and than the modified Smagorinsky model for near-interface treatment. The transfer of energy between the normal turbulent stresses is also well predicted.

The investigation highlights two main advantages of the VMS approach over traditional eddy-viscosity models in this context, namely it implicitly accounts for turbulence decay near the interface without use of damping functions, and it dispenses with modeling the unresolved interfacial that appear in the filtered single-fluid formulation. Future research is needed for interfacial flows featuring more abrupt topology changes (e.g., wave breaking), for which the filtered single-fluid LES equations are solved.

ACKNOWLEDGMENTS

Use of the computing resources at the Swiss Center for Scientific Computing (CSCS), Manno, Switzerland, is gratefully acknowledged. The authors would like to thank Professor S. Banerjee and Dr. V. De Angelis, UCSB, for the helpful discussions. SR was an undergraduate student from Ecole Polytechnique Paris, hosted at ETH Zurich for this work by Professor G. Yadigaroglu.

[1] T. Hughes, A. Oberai, and L. Mazzei, "Les of turbulent channel flows by the variational multiscale method," Phys. Fluids **13**, 1784 (2001).
[2] D. Lakehal, S. Reboux, and P. Liovic, "Subgrid-scale modelling for the LES of interfacial gas-liquid flow," Houille Blanche **6/05**, 1 (2005).
[3] M. Fulgosi, D. Lakehal, S. Banerjee, and V. DeAngelis, "Direct numerical simulation of turbulence in a sheared air-water flow with deformable interface," J. Fluid Mech. **482**, 310 (2003).
[4] B. Perot and P. Moin, "Shear-free turbulent boundary layers. Part 1. Physical insight into near-wall turbulence," J. Fluid Mech. **295**, 199 (1995).
[5] L. Shen, X. Zhang, D. Yue, and G. Triantafyllou, "The surface layer for free-surface turbulent flows," J. Fluid Mech. **386**, 167 (1999).
[6] M. V. Salvetti, Y. Zang, R. L. Street, and S. Banerjee, "Large-eddy simlation of free-surface decaying turbulence with dynamic subgrid-scale models," Phys. Fluids **9**, 2405 (1997).
[7] P. Liovic and D. Lakehal, "Multi-physics treatment in the vicinity of arbitrarily deformable fluid-fluid interfaces," J. Comput. Phys. (in press).
[8] M. Germano, U. Piomelli, P. Moin, and W. Cabot, "A dynamic subgrid-scale eddy viscosity model," Phys. Fluids A **3**, 1760 (1991).
[9] T. Hughes, L. Mazzei, A. Oberai, and A. Wray, "The multiscale formulation of large-eddy simulation: Decay of homogeneous isotropic turbulence," Phys. Fluids **13**, 505 (2001).
[10] J. Holmen, T. Hughes, A. Oberai, and G. Wells, "Sensitivity of the scale partition for variational multiscale large-eddy simulation of channel flow," Phys. Fluids **16**, 824 (2004).
[11] B. Koobus and C. Farhat, "A variational multiscale method for the large-eddy simulation of compressible turbulent flows on unstructured meshes—application to vortex shedding," Comput. Methods Appl. Mech. Eng. **193**, 1367 (2004).
[12] P. Sagaut and V. Levasseur, "Sensitivity of spectral variational multiscale methods for large-eddy simulation of isotropic turbulence," Phys. Fluids **17**, 035113 (2005).
[13] A. Vreman, "The filtering analog of the variational multiscale method in large-eddy simulation," Phys. Fluids **15**, L61 (2003).
[14] K. Walters and S. Bhushan, "A note on spectral energy transfer for multiscale eddy viscosity models in large-eddy simulations," Phys. Fluids **17**, 118102 (2005).
[15] T. J. R. Hughes, G. N. Wells, and A. A. Wray, "Energy transfers and spectral eddy viscosity in large-eddy simulations of homogeneous isotropic turbulence: Comparison of dynamic Smagorinsky and multiscale models over a range of discretizations," Phys. Fluids **16**, 4044 (2004).
[16] V. DeAngelis, P. Lombardi, and S. Banerjee, "Direct numerical simulation of near-interface turbulence in coupled gas-liquid flow," Phys. Fluids **8**, 1943 (1996).
[17] P. Sagaut and M. Germano, "On the filtering paradigm for large-eddy simulation of flows with discontinuities," J. Turbul. **6**, 23 (2005).
[18] P. Liovic and D. Lakehal, "Turbulence-interface interactions in large-scale bubbling processes," Int. J. Heat Fluid Flow (in press).
[19] C. Hartel and L. Kleiser, "Analysis and modelling of SGS motions in near-wall turbulence," J. Fluid Mech. **356**, 327 (1998).
[20] S. Banerjee, D. Lakehal, and M. Fulgosi, "Surface divergence models between turbulent streams," Int. J. Multiphase Flow **30**, 965 (2004).